Catalytic and Stoichiometric Cumulene Formation within Dimeric Group 2 Acetylides

Merle Arrowsmith,[†] Mark R. Crimmin,[‡] Michael S. Hill,*,[†] Sarah L. Lomas,[†] Dugald J. MacDougall,[†] and Mary F. Mahon*,[†]

[†]Department of Chemistry, University of Bath, Claverton Down, Bath BA2 7AY, U.K.

[‡]Department of Chemistry, Imperial College London, Exhibition Road, South Kensington, London SW7 2AZ, U.K.

ⓢ *Supporting Information*

ABSTRACT: A series of β-diketiminate-supported magnesium and calcium acetylide complexes have been synthesized by σ-bond metathesis of magnesium n-butyl or magnesium and calcium amido precursors and a range of terminal acetylenes. The dimeric complexes have been characterized by NMR spectroscopy and X-ray diffraction analysis. The homoleptic bis(amido) and dialkyl complexes $[M\{X-(SiMe_3)_2\}_2(THF)_2]$ (M = Ca, Sr; X = N, CH) have been assessed for the atom-efficient, catalytic head-to-head dimerization of donor-functionalized terminal alkynes into butatrienes and aryl-/silyl-substituted terminal acetylenes into 1,3-enynes. Deuterium labeling studies of the catalytic reactions are suggested to imply that triene formation requires concerted proton delivery and rearrangement via an adjacent methylene group at a bimetallic alkaline-earth species.
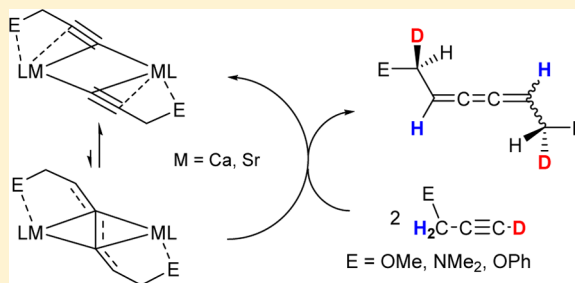
INTRODUCTION

Despite recent and growing interest, the chemistry of σ-organometallic derivatives (i.e., containing a direct metal to carbon σ bond) of the heavier alkaline-earth elements, Ca, Sr, and Ba, is still relatively underdeveloped. Among derivatives of this type, however, σ-bonded acetylides occupy something of a privileged position as the relatively low pK_a of terminal alkynes not only confers thermodynamic stability to σ-bonded group 2 complexes, through charge stabilization in the highly ionic complexes formed upon deprotonation, but also allows facile synthesis through reaction with a suitably basic group 2 precursor.

Originally reported in 1971 by Coles and co-workers,[1] the homoleptic acetylides $[M(C\equiv CPh)_2]_n$ (M = Ca, Sr, Ba) are relatively intractable polymeric materials, which depolymerize slowly upon dissolution in the coordinating solvent tetrahydrofuran. More tractable and soluble materials may be isolated by synthesis of heteroleptic species supported by sterically demanding and lipophilic coligands. Hanusa reported the synthesis of heteroleptic calcium acetylides $[Cp'Ca(C\equiv CR)(THF)]_2$ such as **I** from deprotonation of $RC\equiv CH$ with $[(Cp')Ca\{N(SiMe_3)_2\}(THF)_2]$ (Cp' = $^iPr_4C_5H$).[2] These compounds were shown to be dimeric in the solid state with μ_2-C_α acetylide units asymmetrically bridging the two calcium centers. Despite the presence of the sterically demanding Cp' ligand, solution studies revealed a propensity for these species to undergo undesired Schlenk-like equilibria, limiting studies of these compounds. Ruhlandt-Senge has reported the rational synthesis of a series of homoleptic heavier alkaline-earth acetylides of the formula $[(18\text{-crown-6})M(C\equiv CSiPh_3)_2]$ (**II**–

IV) through the deprotonation of the terminal acetylene with the appropriate group 2 bis(trimethylsilyl)amide $[M\{N-(SiMe_3)_2\}_2]_2$ in the presence of 18-crown-6.[3] Most recently, the same group has discussed the bonding within these and similar species in an attempt to rationalize observed distortions from the more symmetrical geometries predicted by valence shell electron pair repulsion (VSEPR) theory.[4] Combined synthetic and DFT studies concluded that distortions from linearity were facile (of the order of 6 kcal mol^{-1} for a transition from a linear to significantly bent orientation) and could not be ascribed to any one specific structure-determining factor. Rather, the precise details of the bending within acetylide compounds of these readily polarizable metal dications are likely to be dictated by a subtle combination of intraligand steric interactions and crystal-packing effects.

Our interest in these relatively easily accessed σ-bonded organometallic species derives from a focus on how an understanding of structure can be correlated with the observation of well-defined reactivity and, ultimately, can be extrapolated to meaningful structure/activity relationships. We have previously reported a variety of heteroleptic calcium acetylide derivatives supported by a sterically demanding β-diketiminate ligand and have shown that these species generally adopt dimeric formulations, **V**–**IX**, in the solid state.[5] X-ray structural determinations have revealed great variability in the asymmetry of the acetylide with adjustment of the identity of the organic residue of the terminally bonded acetylide. In

I Cp' = (ᶦPr)₄C₅H   II M = Ca; III M = Sr; IV M = Ba   Ar = 2,6-di-*iso*-propylphenyl

R^1 = ⁿBu, **V**
ᵗBu, **VI**
Ph, **VII**
4-MeC₆H₅, **VIII**
(C₅H₄)FeCp, **IX**
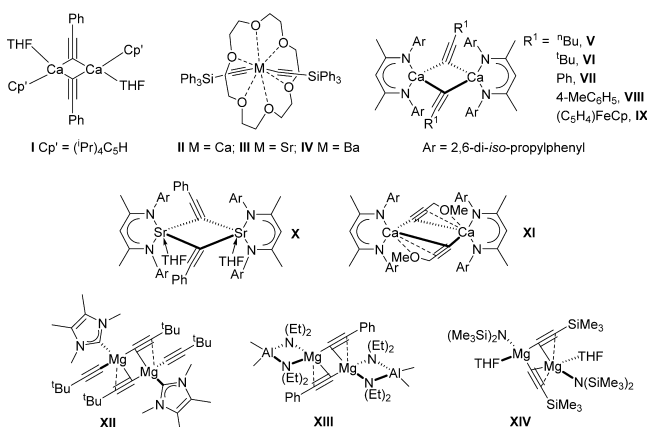
subsequent work, we and others have shown that in the coordinating solvent THF the formation of such symmetrically bridged dimeric complexes may also be perturbed by the coordination of the oxygen-donor solvent to allow the isolation of either monomeric terminal species[6] or asymmetric dimers including the unique heteroleptic strontium acetylide compound **X**.[7] For symmetrically bridged acetylide compounds, the extent of this "side-on" interaction between the C≡C unit and the calcium center may be defined and quantified in terms of the M−C$_\alpha$−C$_\beta$ (θ) and the M′−C$_\alpha$−C$_\beta$ (ϕ) angles (Figure 1)
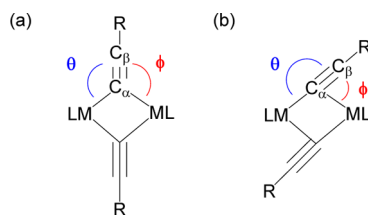
Figure 1.

between two extremes; either symmetrical where the acetylide unit lies perpendicular to the metal−metal vector, $\theta = \phi$, or "completely side-on", in which case $\theta - \phi = 90°$. On the basis of these observations we have speculated that higher values of $\theta - \phi$ enhance a, albeit relatively minor, dissipation of negative charge over both alkynyl carbon centers.[5] Due to a coordinative interaction between a methoxy substituent and calcium, a compound containing the terminal acetylide ligand [CH₃OCH₂C≡C]⁻ and adopting a similar dimeric constitution, compound **XI**, provided the most asymmetric structure yet reported, in which $\theta - \phi$ was 79.9°.[8] Furthermore, this latter species displayed a remarkably specific C−C coupling reaction upon the addition of further equivalents of terminal acetylene (Scheme 1). We speculated that this reactivity could

Scheme 1
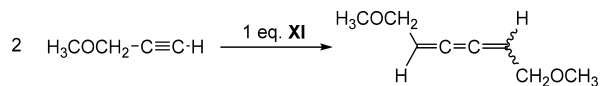
be rationalized as resulting from a reduction in the mutual repulsion of the C$_\alpha$ centers within the dimeric structure and the formation of a transition state in which the C₄ bridging bis(acetylide) fragment has significant butatriene diyl character during protonolysis. We have recently speculated that similar considerations of substrate/ligand polarization and cation

polarizability may dictate the reactivity of the group 2 elements in alkene heterofunctionalization catalysis.[9] Catalytic dimerization of terminal alkynes has already been reported using a variety of similarly d⁰ f-element cyclopentadienyl-supported precatalysts of both the rare earths (Sc,[10] Y,[11,12b] La, Ce,[12] Lu[13]) and the actinides (Th, U[14]). In all cases, however, the products of these reactions were the thermodynamically more stable 1,3-enynes. In this contribution, we explore the generality of the calcium-catalyzed acetylene coupling reactivity illustrated in Scheme 1 and describe our attempts to extend this reactivity to other members of the alkaline-earth elements.

■ RESULTS AND DISCUSSION

Synthesis of Magnesium and Calcium Acetylides. The β-diketiminato magnesium and calcium complexes **1−10** were synthesized by addition of 1 molar equiv of the relevant terminal acetylene to the appropriate magnesium or calcium amide complex [LM{N(SiMe₃)₂}(THF)$_n$] (L = [HC{(Me)-CN(2,6-ⁱPr₂-C₆H₃)}₂]; M = Mg, n = 0; M = Ca, n =1) in benzene or toluene, respectively (Scheme 2). For the calcium

Scheme 2

M = Mg, n = 0; M = Ca, n = 1
Ar = 2,6-di-*iso*-propylphenyl

M = Mg, **1**: R^1 = ⁿBu   **5**: R^1 = p-tol
2: R^1 = ᵗBu   **6**: R^1 = CH₂OCH₃
3: R^1 = Cy   **7**: R^1 = CH₂OPh
4: R^1 = Ph   **8**: R^1 = CH₂N(CH₃)₂

M = Ca, **9**: R^1 = CH₂OPh
10: R^1 = CH₂N(CH₃)₂
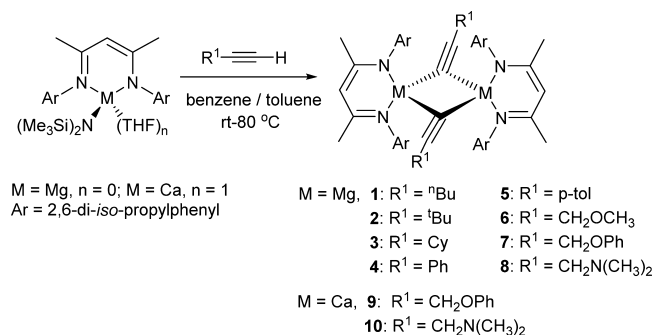
complexes σ-bond metathesis occurred spontaneously at room temperature and NMR-scale reactions showed complete conversion within the first point of analysis. The slightest excess of the acetylene precursor led to protonolysis of the β-diketiminate ligand and the formation of highly insoluble polymeric calcium bis(acetylide) materials. Synthesis of the heteroleptic magnesium acetylides required heating at 60 °C for 24 h, except in the case of the bulkier *tert*-butylacetylene derivative, which required heating at 80 °C for 2 days for the reaction to proceed to completion. Protonolysis of the β-diketiminate ligand in the presence of excess acetylene was not observed unless the reaction mixture was heated above 80 °C. The compounds were either crystallized directly from the reaction mixture or recrystallized from toluene and isolated as highly air- and moisture-sensitive colorless crystalline solids. Complexes were sufficiently soluble in d_8-toluene to provide ¹H and ¹³C NMR data, apart from the magnesium derivatives of *tert*-butylacetylene, phenylacetylene, and the dimethylamino-substituted acetylene Me₂NCH₂C≡CH, compounds **2**, **5**, and **8**, which required the more coordinating solvent d_5-pyridine for the acquisition of meaningful ¹³C NMR data. Four 6H doublet resonances attributed to the diastereotopic methyl groups of the 2,6-diisopropylphenyl substituents, as well as two corresponding methine septets, were observed in the ¹H NMR spectra of all four toluene-soluble magnesium compounds, indicative of the maintenance of a dimeric constitution in noncoordinating solvents as well as, most likely, a hindered rotation of the N-aryl substituents of the β-diketiminate ligands.

Table 1. ^{13}C NMR Resonances of the C_α and C_β Acetylide Carbons for Complexes 1−10

	^{13}C NMR shift (ppm)									
	1^a	2^b	3^b	4^b	5^b	6^a	7^a	8^b	9^c	10^c
MC_α≡C_β	121.0	120.1	115.4	122.0	125.4	120.4	120.1	112.9	148.6	135.0
MC_α≡C_β	112.2	103.5	105.8	111.2	115.3	115.6	115.1	104.7	106.3	102.8

^{a}In d_8-toluene. ^{b}In d_5-pyridine. ^{c}In C_6D_6.
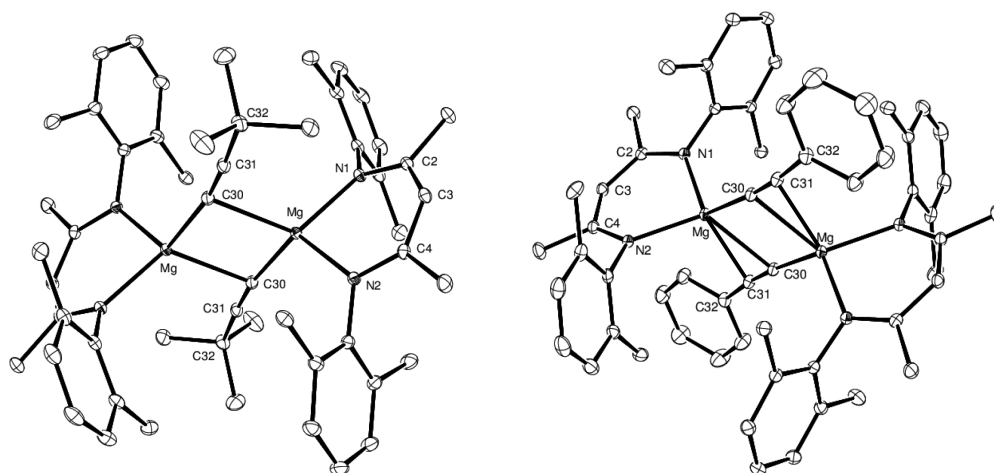
Figure 2. ORTEP representations of (left) complex 2 and (right) complex 4. Thermal ellipsoids are given at the 20% probability level. Hydrogen atoms and isopropyl methyl groups are removed for clarity. Symmetry transformations used to generate equivalent atoms in 2: −x + 1, −y, −z + 1. Symmetry transformations used to generate equivalent atoms in 4: −x + 2, −y + 1, −z.

In contrast, the corresponding methyl environments of compounds 9 and 10 and those of the previously reported dimeric calcium derivatives V−IX[5] appeared as a single pair of doublet resonances. These observations are consistent with a greater degree of steric congestion in complexes containing the lighter and smaller alkaline-earth element. Similarly to its *tert*-butylacetylide analogue,[5] however, variable-temperature NMR experiments on the calcium phenyl propargyl ether derivative 9 showed signs of hindered rotation at temperatures below 228 K. The low solubility of the compound at reduced temperatures prevented quantification of this rotation barrier. In contrast, the dimethylamino-1-propyne derivative 10 did not display any signs of hindered rotation down to 198 K. This may be counterintuitive, given that the dimethylamino functionality should induce higher steric hindrance than the corresponding phenoxy group, but can be ascribed to the additional metal coordination provided by the ether oxygen atom within dimer 9 (see Solid-State Characterization). NOESY experiments carried out at room temperature in d_8-toluene also showed an interaction between the ortho protons of the O-phenyl ring with the isopropyl methine and the β-CH backbone protons of the β-diketiminate ligand, suggesting retention of the dimeric nature of the complex in solution. No NOESY peaks were observed between the resonances of the spectator ligand and the acetylide fragment in the case of the dimethylamino-substituted analogue 10.

Table 1 shows the ^{13}C NMR resonances of the C_α and C_β acetylide carbons for each of the complexes, which were all confirmed through independent HMBC experiments. The C_α resonance was shifted ca. 50 ppm downfield from those of the parent acetylenes and showed no significant trend in the chemical shift over the whole range of magnesium complexes independent of the NMR solvent (δ^{13}C 115.4−125.4 ppm). The C_β ^{13}C NMR shift of these complexes only experienced a ca. 10

ppm downfield shift in comparison to that of the alkyne precursors and varied significantly according to the inductive nature of the acetylenic substituent: in d_8-toluene the more electron-withdrawing methoxymethyl and phenoxymethyl functionalities of compounds 6 and 7 led to resonances farthest downfield (δ^{13}C ca. 115 ppm), while the *n*-butyl functionality of complex 1 induced a slightly more upfield shift to around δ^{13}C 112 ppm. The C_β resonances of 2−5 and 8 recorded in d_5-pyridine displayed a similar trend, with the aryl substituents inducing a downfield shift of ca. 10 ppm in comparison to the alkyl substituents. For comparison Roesky and co-workers reported C_α and C_β NMR shifts in C_6D_6 at δ^{13}C 130.1 and 117.5 ppm for their NHC-supported magnesium bis(*tert*-butylacetylide) dimer XII,[7] while Chang et al. synthesized a series of heteroleptic magnesium acetylides supported by chelating dialkyldiamidoaluminate ligands, including compound XIII, with C_β ^{13}C NMR shifts in C_6D_6 ranging from 97.9 to 111.4 ppm, similar to those observed herein.[15] In the case of calcium complexes 9 and 10, the downfield shift induced by metal ligation upon the C_α resonance was observed to be much more significant and more dependent on the nature of the acetylide ligand than for the analogous magnesium complexes (9, δ^{13}C 148.6 ppm; 10, δ^{13}C 135.0 ppm). This may be due to the more ionic nature of the Ca−C bond in comparison to the more covalent Mg−C bond. The C_α chemical shifts for the analogous β-diketiminato calcium 1-hexynyl and *tert*-butylacetylide dimers V and VI in d_8-toluene (δ^{13}C 125.5 and 125.3 ppm, respectively) were reported to be somewhat farther upfield and closer to those observed for magnesium complexes 1−8. In contrast, the C_β resonances for 9 and 10 (δ^{13}C 106.3 and 102.8 ppm, respectively) seem much less affected by the nature of the metal center, although comparison with the analogous magnesium phenyl propargyl ether and dimethylamino-3-propyne deriva-
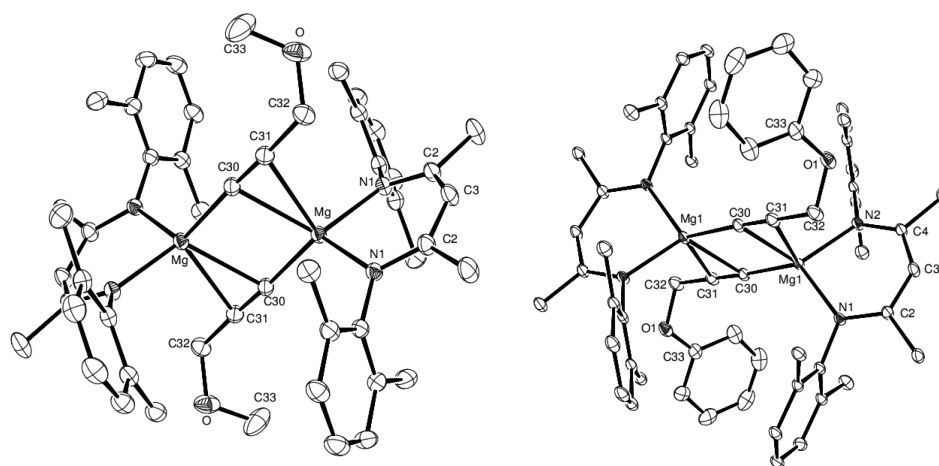
Figure 3. ORTEP representations of (left) compound **6** and (right) compound **7**. Thermal ellipsoids are given at the 20% probability level. Hydrogen atoms and isopropyl methyl groups are removed for clarity. Symmetry transformations used to generate equivalent atoms in **6**: x, $-y + 1$, z; $-x + 1$, $-y + 1$, $-z + 1$; $-x + 1$, y, $-z + 1$; x, $-y$, z. Symmetry transformations used to generate equivalent atoms in **7**: $x + 1$, $-y + 1$, $-z + 1$; $-x$, $-y$, $-z + 2$; $-x$, $-y$, $-z + 1$.

Table 2. Selected Bond Lengths and Angles for Compounds 2, 4, 6, 7, XI, 9, and 10

	2	4	6	7	XI[7]	9	10
M−C30	2.1908(12)	2.1740(16)	2.151(3)	2.162(2), 2.157(2)	2.498(2), 2.489(3)	2.4841(18)	2.505(2)
M−C30′	2.3051(12)	2.3485(15)	2.340(3)	2.345(2), 2.370(2)	2.666(3), 2.697(3)	2.6788(16)	2.536(2)
M−C31′	2.8080(12)	2.6705(16)	2.528(4)	2.518(2), 2.505(2)	2.721(3), 2.742(2)	2.7286(17)	2.866(2)
M−O					2.507(2), 2.469(2)	2.7410(12)	
C30−C31	1.2216(17)	1.222(2)	1.227(4)	1.223(3), 1.218(3)	1.217(4), 1.212(4)	1.216(2)	1.214(3)
N1−M−N2	92.47(4)	91.63(5)	93.33(10)	93.51(6), 94.50(7)	83.06(7), 80.22(7)	79.72(4)	81.69(6)
M−C30−M′	88.90(4)	92.32(6)	92.80(12)	93.00(9), 93.83(8)	98.38(9), 99.57(9)	101.84(6)	90.76(7)
C30−M−C30′	91.10(4)	87.68(6)	87.20(13)	87.00(8), 86.17(8)	81.62(9), 80.43(9)	78.16(6)	89.24(7)
M−C30−C31 (θ)	170.00(10)	175.72(13)	176.9(3)	176.4(2), 175.4 (2)	172.1(2), 178.4(2)	175.00(17)	176.33(19)
M′−C30−C31 (ϕ)	101.04(9)	91.24(10)	84.1(2)	83.45(17), 81.74(16)	79.5(2), 79.2(2)	79.30(11)	92.86(16)
C30−C31−C32	176.10(13)	174.75(16)	177.4(4)	179.1(3), 177.9(3)	170.4(3), 170.0(3)	176.54(18)	178.7(2)

tives **7** and **8** is precluded due to the different NMR solvents used to record the spectra in each case.

Solid-State Characterization. Although all eight of the magnesium compounds provided crystals suitable for single-crystal X-ray analysis, data were only collected for compounds **1**, **2**, **4**, and **6**−**8**. Unfortunately data for the *n*-hexyne and 3-dimethylamino-1-propyne derivatives, compounds **1** and **8**, were unsatisfactory (R1 >12%), precluding any detailed discussion of bond lengths and angles (see Figures S1 and S2 in the Supporting Information for ORTEP representations of **1** and **8**). The connectivity of all six crystallographically characterized species was, however, unambiguous and indicated dimeric structures irrespective of the precision of the structural data. The structures of the *tert*-butyl- and phenylacetylide complexes **2** and **4** are depicted in Figure 2, and the structures of the methyl and phenyl propargyl ether magnesium compounds **6** and **7** are illustrated in Figure 3. Details of the X-ray analyses and selected bond length and angle data for all magnesium acetylides are provided in Table S1 (Supporting Information) and Table 2, respectively. The asymmetric unit of complex **7** is composed of two structurally distinct molecules. For all six magnesium complexes, dimerization occurs in a similar manner through μ_2-bridging terminal acetylide interactions. While the *tert*-butylacetylene, phenylacetylene, and phenyl propargyl ether derivatives **2**, **4** and **8**, present molecular D_2 symmetry, the methyl propargyl ether derivative **6** displays a further mirror plane including the Mg_2C_2 bridging core,

providing D_{2h} symmetry and causing the methoxy fragment to be disordered over two positions. While the calcium analogue **XI** featured additional coordination to the metal center via the oxygen atom of the bridging methyl propargyl ether ligand, no such interaction is seen in the magnesium derivative. This may be ascribed to the much shorter metal–metal separation in the magnesium dimer (3.2548(19) Å) in comparison to that in complex **XI** (3.9101(5)−3.9623(6) Å),[8] which enables the less constrained methoxy substituent to coordinate to the second calcium center. As had already been observed with analogous dimeric β-diketiminate calcium acetylides[5] and related acetylides,[16] the four-membered planar Mg_2C_2 bridging cores in these complexes are slightly asymmetric. The Mg−C30 bond lengths range from 2.151(3) to 2.1740(16) Å, similar to those observed in the phenyl- and *p*-tolylacetylide magnesium aluminate dimers reported by Chang et al. (2.157(6)−2.192(2) Å), which also feature an asymmetric alkynyl bridging mode.[15] The Mg′−C30 distances (2.340(3)−2.370(2) Å), however, are significantly longer than any reported to date in other crystallographically characterized μ_2-acetylide magnesium dimers. This is likely to be a consequence of the high steric demands of the supporting β-diketiminate ligand, which forces the two magnesium centers farther apart, and it is notable that the Mg··· Mg′ distances in complexes **2**, **4**, **6**, and **7** (3.1496(7)−3.3106(12) Å) are by far the longest reported to date for acetylide-bridged magnesium dimers (vide infra). In all cases the linear ethynyl moiety forms

Table 3. Bridging Angles (deg) and Bond Lengths (Å) in Complexes 2, 4, 6, 7, and XII–XIV

	2	4	6	7	XII[7]	XIII[15]	XIV[17z]
$\theta - \phi$	69.0	84.5	92.8	93.0, 93.7	79.7	58.5	67.2
Mg- - -Mg′	3.1496(7)	3.2643(9)	3.2548(19)	3.2721(13), 3.3106(12)	3.0943(9)	3.001(2)	3.088(2)
Mg′–C$_\beta$	2.8080(12)	2.6705(16)	2.528(4)	2.519(2), 2.504(2)	2.708(2)	2.8417(3)	2.760(4)
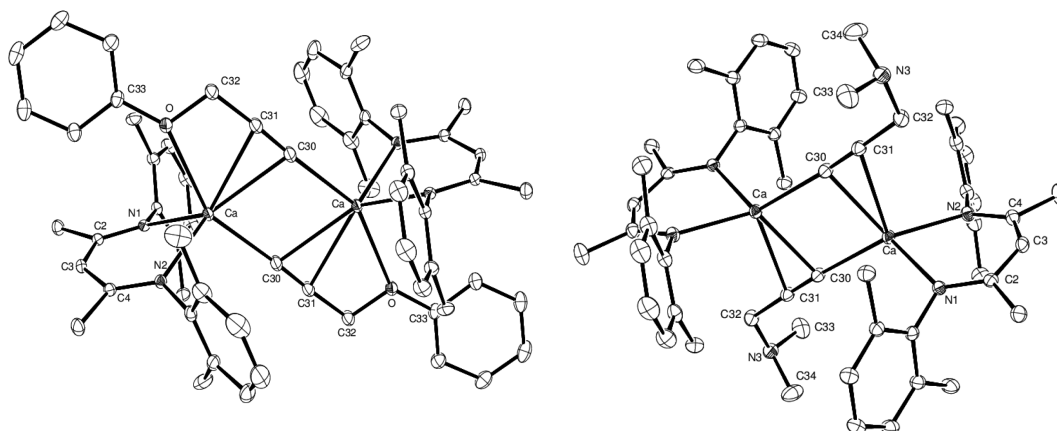
Figure 4. ORTEP representations of (left) compound **9** and (right) compound **10**. Thermal ellipsoids are given at the 20% probability level. Hydrogen atoms and isopropyl methyl groups are removed for clarity. Symmetry transformations used to generate equivalent atoms in **9**: −x + 1, −y, −z. Symmetry transformations used to generate equivalent atoms in **10**: −x, −y + 1, −z; −x, −y + 2, −z + 1.

an acute angle with the Mg–Mg vector, with relatively short Mg′–C31 distances (2.505(2)–2.6705(16) Å), except for the *tert*-butyl-substituted acetylide **2** (2.8080(12) Å), suggesting a potential π interaction between the C–C triple bond and the metal center. Although a wide variety of magnesium acetylide complexes have been reported previously, only a few present a bridging acetylide unit and, among these, most display a symmetrical bridging core in which the alkynyl ligand lies perpendicular to the Mg–Mg vector and acts as a formal one-electron donor.[10,17] In a manner similar to that for our previous analysis of β-diketiminate calcium acetylide dimers,[5,8] the bridging asymmetry in complexes **2**, **4**, **6**, and **7** may be quantified in terms of the difference between the Mg–C30–C31 (θ) and Mg′–C30–C31 (ϕ) angles (see Table 3). Apart from the *tert*-butylacetylide derivative **2**, the magnesium compounds all provide $\theta - \phi$ values close to 90° (84.5–93.7°), suggestive of a high degree of π interaction. Similar bonding arrangements have previously been observed in a handful of other dimeric magnesium acetylide species, including the NHC-supported complex [{(MeCNMe)$_2$C:}(^{t}BuC≡C)-Mg(μ_2-C≡C^{t}Bu)]$_2$ (**XII**),[7] the phenylacetylide magnesium aluminate complex [{Me$_2$Al(NEt$_2$)$_2$}Mg(μ_2-C≡CPh)]$_2$ (**XIII**),[15] and the unusual noncentrosymmetric dimer [{(Me$_3$Si)$_2$N}(THF)Mg(μ_2-C≡CSiMe$_3$)]$_2$ (**XIII**).[17a] For comparison, the $\theta - \phi$ values and the Mg- - -Mg′ and Mg′–C$_\beta$ distances for these three complexes are presented in Table 3 alongside those of the β-diketiminate magnesium complexes **2**, **4**, **6**, and **7**. Higher $\theta - \phi$ values correlate with shorter Mg′–C$_\beta$ distances and are thus indicative of a stronger C≡C π interaction with the metal centers. It is also of interest to note that the $\theta - \phi$ values within complexes **XII–XIV** and the values described herein in general increase with increasing steric demands of the terminal supporting ligands, such that the two magnesium centers are forced further apart, allowing for a more favorable side-on interaction between the magnesium dications and the ethynyl moiety.

Crystals of the two calcium acetylide complexes **9** and **10** suitable for X-ray diffraction analysis were isolated from recrystallizations in toluene. The results of these experiments are depicted in Figure 4. Details of the analyses and selected bond lengths and angles are given in Table S1 (Supporting Information) and Table 2, respectively. As with previously reported β-diketiminato calcium acetylides, both complexes are dimeric in the solid state. Coordination at the metal centers is provided by the bidentate β-diketiminate ligands as well as the bridging C30 and C31 acetylide carbon atoms. While in complex **10** the potential nitrogen donor center of the dimethylamino moiety is oriented away from the second calcium center, the phenoxy moiety in complex **9** provides additional coordination through the ether oxygen atom, just as in the methyl propargyl ether analogue **XI**.[8] Both complexes present molecular D_2 symmetry and an asymmetric planar Ca$_2$C$_2$ bridging core. However, the structurally very similar complexes **XI** and **9** display several differences in their bond lengths and angles. The larger size of the phenyl versus the methyl substituent on the metal-bound oxygen atom induces a widening of the Ca- - -Ca′ distance by ca. 0.07 Å (**9**, 4.0095(5) Å; **XI**, 3.9101(5)–3.9623(6) Å) as well as a significant decrease in the N1–Ca–N2 and C30–Ca–C30′ bite angles (**9**, N–Ca–N = 79.72(4)°, C–Ca–C 78.16(6)°; **XI**, N–Ca–N = 80.22(7)–83.06(7)°, C–Ca–C = 80.43(9)–81.62(9)°). In the methoxy derivative **XI**, the strong interaction between the metal center and the oxygen atom (Ca–O = ca. 2.49 Å) caused a significant deviation from linearity in the alkynyl moiety (C30–C31–C32 = ca. 170°). The lengthening of the Ca–O bond length in complex **9** (2.7410(12) Å), however, also enables the acetylide fragment to preserve its linearity (C30–C31–C32 = 178.7(2)°). In the dimethylamino derivative no interaction between N3 and the second calcium center of the dimer is observed. This may be ascribed to the higher steric demands of the dimethylamino substituent in comparison to analogous methoxy and phenoxy derivatives, in conjunction with the higher affinity of the group 2 dication toward ether

Table 4. Bridging Angles (deg) and Bond Lengths (Å) in Complexes 9, 10, VI, VII, and XI

	9	10	VI[5]	VII[5]	XI[8]
$\theta - \phi$	83.47	92.6	46.4	76.2	95.7, 99.2
Ca- - -Ca$'$	4.0095(5)	3.5887(5)	3.5481(2)	3.5735(3)	3.9101(5), 3.9623(6)
Ca$'$−C$_\beta$	2.7286(17)	2.866(2)	3.167(2)	2.9403(3)	2.721(3), 2.742(2)

rather than tertiary alkylamine coordination. The $\theta - \phi$ value of 92.6°, however, is still indicatative of a high degree of π donation, comparable to that in complexes **9** and **10**, despite a Ca- - -Ca$'$ distance of 3.5887(5) Å, more commensurate with the *tert*-butyl- and phenylacetylene derivatives, which display much lower $\theta - \phi$ values (see Table 4).

Group 2 Mediated Coupling of Terminal Acetylenes Containing Donor Appendages. We have previously reported that the heteroleptic calcium triazenide complex $[\{(2,6\text{-}^i\text{Pr}_2\text{C}_6\text{H}_3)_2\text{N}_3\}\text{Ca}\{\text{N}(\text{SiMe}_3)_2\}(\text{THF})_2]$ (**XV**) is an efficient precatalyst for the catalytic dimerization of methyl propargyl ether to the butatriene product $[\text{MeOCH}_2\text{CH}{=}\text{C}{=}\text{C}{=}\text{CHCH}_2\text{OMe}]$ under relatively mild conditions (Scheme 3;

Scheme 3

Table 5, entry 1).[8] This catalytic protocol has now been extended to a wider range of alkaline-earth precatalysts, and alkyne substrate types and the results are presented in Tables 5 and 6. For complex **XV**, it was observed that turnover was
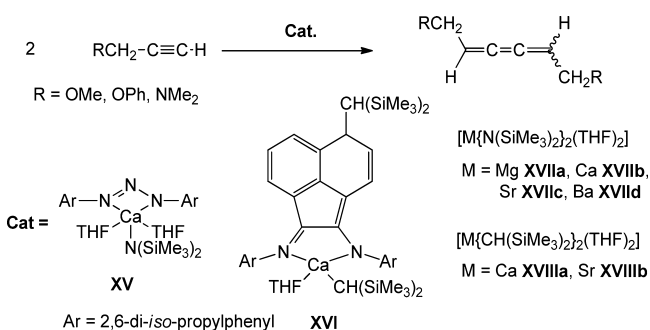
Table 5. Precatalyst (5 mol %) Screening for the Dimerization of Methyl Propargyl Ether

entry	precatalyst	temp (°C)	time (h)	NMR yield (%)
1	**XV**[a]	75	48	91
2	**XVI**[b]	80	48	12
3	**XVIIa**[c]	100	17	<0.5
4a	**XVIIb**[c]	100	17	57
4b	**XVIIb**[c]	100	48	95
5	**XVIIc**[c]	100	17	6
6	**XVIId**[c]	100	17	<0.5
7	**XVIIIa/b**[c]	100	24	<2

[a]6.25 mol % in C_6D_6. [b]In C_6D_6. [c]In d_8-toluene + 20 mol % THF.

Table 6. Influence of Added THF on the Catalytic Coupling of Methyl Propargyl Ether in d_8-Toluene after 1 h at 100 °C with 5 mol % of XVIIb

added THF (mol %)	0	10	20	30	60	100	>500
butatriene NMR yield (%)	10	18	20	17	16	14	<2

accompanied by significant amounts of ligand redistribution to yield the homoleptic species $[\{(2,6\text{-}^i\text{Pr}_2\text{C}_6\text{H}_3)_2\text{N}_3\}_2\text{Ca}(\text{THF})_2]$ and, presumably, polymeric $[\text{Ca}\{\text{C}{\equiv}\text{CCH}_2\text{OMe}\}_2]_n$. Conversely, the much more sterically encumbered BIAN calcium alkyl derivative **XVI**[18] proved very sluggish at 80 °C (ca. 12% conversion after 2 days) and was also prone to ligand redistribution processes at higher temperatures (Table 5, entry 2). Attempts to catalyze the reaction using the simple homoleptic calcium amide precatalyst **XVIIb** in d_8-toluene were limited to a maximum of eight turnovers using slightly more forcing conditions (90 °C, 48 h), the main limiting factor being the lack of solubility of the presumed active catalyst, $[\text{Ca}\{\text{C}{\equiv}\text{CCH}_2\text{OMe}\}_2]_n$. Any increase in catalyst loading led to even lower solubility and turnover numbers. While changing the solvent to the more coordinating d_8-THF improved the solubility, it also resulted in notable suppression of activity (Table 6). Conversely, addition of 20 mol % of THF to the reaction mixture in d_8-toluene dramatically improved catalyst solubility as well as allowing the reaction to proceed to near quantitative conversion within 48 h at 100 °C using 5 mol % loading of **XVIIb** (Table 5, entry 4b). Any increase above this temperature, however, led to the precipitation of dark brown insoluble materials and a drastic loss of activity. We suggest that this marked dependence upon THF loading represents a compromise between sufficient donor solvent to maintain catalyst solubility and a displacement of the solution equilibrium away from the dimeric constitution required for catalytic triene formation (vide infra).

Equivalent experiments using the series of analogous group 2 bis(amides) **XVIIa−d** revealed the calcium compound to be by far the best precatalyst (Table 5, entries 3−6). Virtually no conversion to the coupled product was observed in the cases of magnesium and barium even after prolonged periods of heating at 100 °C, while the strontium complex displayed significantly lower activity than calcium. This order of reactivity correlates with that determined for group 2 catalyzed intramolecular hydroamination reactions with complexes **XVIIa−d** but diverges from that established for the intermolecular hydroamination of activated alkenes, in which the strontium precatalyst provided greater activity than the calcium analogue. We have previously reasoned that these latter observations are a consequence of a significant entropic advantage provided by the larger and more labile Sr^{2+} center.[19] Using the related dialkyl precatalysts **XVIIIa/b** under these conditions, however, led to a significant decrease in solubility of the active bis(acetylide) species and suppression of catalytic activity (Table 5, entry 7).

With these observations in hand, the reaction was successfully scaled up using 0.5 g of methyl propargyl ether, 10 mol % of **XVIIb**, and 40 mol % of THF in 9 mL of toluene at 100 °C. Although filtration of the reaction mixture and vacuum transfer of volatiles yielded a ca. 0.03 M stock solution of $[\text{MeOCH}_2\text{CH}{=}\text{C}{=}\text{C}{=}\text{CHCH}_2\text{OMe}]$ in toluene, the butatriene derivative could not be isolated, as it seemed to form an azeotrope with toluene. Although attempts to coordinate $[\text{MeOCH}_2\text{CH}{=}\text{C}{=}\text{C}{=}\text{CHCH}_2\text{OMe}]$ to either Rh(I) or Ir(I) centers indicated a predominance of the *E*

Table 7. Scope of Calcium-Mediated Terminal Alkyne Coupling in d_8-Toluene

Entry	Substrate	Product(s)	Catalyst (mol%)	THF (mol%)	Temp. (°C)	Time (h)	NMR yield (%)
1	MeOCH₂C≡CH	MeO⌇⌇⌇OMe	**XVIIb** (5)	20	100	48	>99
2	PhOCH₂C≡CH	PhO⌇⌇⌇OPh	**XVIIb** (5)	20	100	3 days	5
3	Me₂NCH₂C≡CH	Me₂N⌇⌇⌇NMe₂	**XVIIb** (5)	20	100	3 days	5
4a			**XVIIa/d** (5)	20	160	21	0
4b			**XVIIb** (5)	20	160	21	<1
4c		Ph—≡—...Ph—≡—	**XVIIc** (5)	20	160	21	1
4d	PhC≡CH	Ph, **XVIIIa** 9:1; **XVIIIb** 4:1, Ph	**XVIIIa** (5)	20	160	48	10
4e			**XVIIIb** (5)	20	160	48	12
4f			**XVIIIa** (5)	b	160	3 days	90
4g			**XVIIIb** (5)	b	160	3 days	87
5	(p-tol)C≡CH	p-tol—≡—; p-tol—≡—p-tol 1:2	**XVIIIa** (10)	b	160	9 days	80
6	(ⁱPr)₃SiC≡CH	(ⁱPr)₃Si—≡—Si(ⁱPr)₃	**XVIIIa** (10)	b	160	9 days	35
7	CyC≡CH	–	**XVIIIa** (10)	b	170	4 days	0
8	ⁱBuC≡CH	–	**XVIIIa** (10)	b	170	4 days	0
9	ⁿBuC≡CH	ⁿPr⌇⌇⌇ⁿPr	**XVIIIa** (10)	b	170	4 days	3

[a] Stoichiometric reaction: **XVIIb** and acetylene in a 1/4 ratio. [b] Reactions carried out in 9/1 toluene/THF mixture.

isomer in this solution, the E/Z stereochemistry of the triene products could not be ascertained with any meaningful degree of confidence. The activation barriers to internal rotation of substituted butatriene derivatives have been estimated to be as low as 20 kcal mol^{-1}, commensurate with the energies associated with internal rotation about peptide C−N bonds.[20] It is, thus, highly probable that under the high-temperature conditions required for catalytic synthesis the products are prone to some degree of thermal equilibration between the two possible geometric isomers, irrespective of the initial substitution pattern.

We have previously postulated that the high $\theta - \phi$ value observed in dimer **XI**, aided by the coordination of the ether moiety to the adjacent calcium center, leads to a dissipation of negative charge over the two acetylide carbon atoms, leading to a decrease in repulsion between the two C_α centers and consequent promotion of C−C coupling.[8] With this in mind, the catalytic dimerization reactions of phenyl propargyl ether and 3-dimethylamino-1-propyne were attempted using the same conditions identified for successful methyl propargyl ether coupling. In both cases analysis by ^{1}H NMR spectroscopy confirmed the clean formation of the desired butatriene products, each of which displayed characteristic triplet and doublet resonances (1,6-diphenoxy-2,3,4-hexatriene, δ_H 6.44 (t, 2H), 5.10 ppm (d, 4H); 1,6-bis(dimethylamino)-2,3,4-hexatriene, δ_H 5.92 (t, 2H), 5.12 ppm (d, 4H)). Conversions, however, remained stoichiometric even after prolonged heating at 100 °C (Table 7, entries 2 and 3). In both cases catalysis was hampered by the formation of dark red precipitates which were insoluble in hydrocarbon and ether solvents. The color of the precipitates was reminiscent of that reported for various cyclopentadienyl lanthanum, neodymium, and samarium 1,4-diphenylbutatriene diyl dimers reported by Marks and Evans.[21]

The materials resulting from the current group 2 based processes are, thus, tentatively ascribed to the formation of stable calcium butatriene diyl complexes.

To probe the mechanism of butatriene formation, the behavior of calcium complex **XI** was studied by variable-temperature NMR spectroscopy. Surprisingly, the dimer proved immune to ligand redistribution up to 110 °C in d_8-toluene, presumably due to additional stabilization afforded by coordination of the ether moiety. Furthermore, ^{13}C{^{1}H} and HMBC NMR experiments evidenced no shift in the acetylide carbon resonances toward a butatriene diyl intermediate. Similar observations were made for the phenyl propargyl ether derivative **9**, whereas the 3-dimethylamino-1-propynyl complex **10** displayed signs of Schlenk-type equilibration above 90 °C. Upon addition of 2 molar equiv of methyl propargyl ether to a d_8-toluene solution of **XI**, small amounts of the butatriene coupling product (<5%) were observed after 10 min at 50 °C, together with some protonation of the β-diketiminate ligand. It thus appears that acetylene dimerization only occurs in the presence of excess acetylene. Comparable observations have already been reported for group 2 catalyzed intramolecular hydroamination reactions, in which an isolated magnesium amidoalkene complex has been observed to undergo cyclization only upon addition of a further 1 equiv of amine substrate.[22] In related hydroamination/cyclization studies using a variety of alkaline-earth catalysts we and others have also reported large kinetic isotope effects, leading to the proposal that catalytic turnover must proceed via a concerted insertion/protonolysis step.[8,17b,18,23] We suggest, therefore, that a similar concerted mechanism is also operative in the present case, which as a result prevents isolation or even observation of the putative calcium butatriene diyl intermediate.

To probe this hypothesis, kinetic experiments on the dimerization of methyl propargyl ether and its deuterated equivalent MeOCH₂C≡CD (0.8 M) were carried out at 100 °C in 0.5 mL of d_8-toluene using 10 mol % of **XVIIb** and 40 mol % of THF and monitored at regular intervals by ^{1}H NMR spectroscopy. The results could be fitted to zero-order kinetics over 2 half-lives with a rate constant of 0.122 M h⁻¹, after which the reaction slowed down considerably as the substrate concentration decreased below that of THF (Figure S4, Supporting Information). Dimerization of the deuterated species occurred at a much slower rate (k_D = 0.025 M h⁻¹), yielding a large kinetic isotope effect of k_D/k_H = 4.8.

^{1}H NMR spectroscopic analysis of the deuterated coupling product also provided surprising insight into the mechanism of formation of the butatriene species: rather than the expected 4H allylic resonance at 5.24 ppm, two mutually coupled resonances were observed at 6.71 and 5.24 ppm in a 1/1 ratio (Figure S5, Supporting Information). The ^{2}H NMR spectrum displayed two resonances at 0.02 and 5.27 ppm corresponding to the byproduct of the initial catalyst activation, $DN(SiMe_3)_2$, along with the deuterated butatriene product [MeOCDHCH=C=CHCDHOMe], respectively (Scheme 4). Further-more, ¹³C{¹H} NMR data confirmed the exclusive deuteration of the allylic position, with a CDH triplet resonance at 90.7 ppm ($^2J_{C-D}$ = 25.6 Hz) and a vinylic CHCD₂ signal at 123.5 ppm broadened by ^3J coupling to deuterium. Thus, the positions of deuteration of the product indicated a further subtlety in the mechanism of alkyne coupling, which we tentatively suggest may be accounted for by the assembly of a protonolysis transition state such as that depicted in Figure 5.
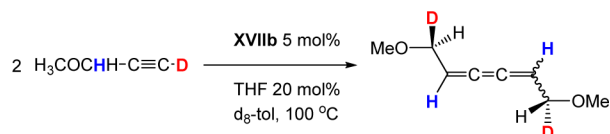
Scheme 4
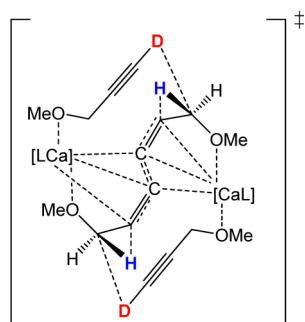
Figure 5. Suggested protonolysis transition state accounting for the selective incorporation of deuterium into the triene methylene group.

In this case formation of the butatriene fragment occurs via a concerted mechanism involving a dimeric calcium acetylide species, which undergoes synchronous acetylene-assisted butatriene diyl formation, isomerization, and protonolysis.

Group 2 Mediated Coupling of Terminal Acetylenes without Donor Appendages. To assess whether acetylenes without a donor functionality may undergo similar group 2 catalyzed coupling reactions, a NMR-scale reaction of phenyl-acetylene with 5 mol % of **XVIIb** and 20 mol % of THF was

conducted in d_8-toluene and monitored at increasing temperatures by ^{1}H NMR spectroscopy. While quantitative proto-nolysis of hexamethyldisilazane occurred spontaneously at room temperature, no further reactivity was observed up to 100 °C. Although increasing the temperature to 160 °C for 21 h caused the reaction mixture to turn dark red, the corresponding ^{1}H NMR spectrum showed less than 1% conversion to a single product. This species, characterized by two doublet resonances at 5.67 and 6.46 ppm forming an AB spin system, was identified as the Z isomer of [PhC≡CCH=CHPh] ($^3J_{cis}$ = 11.7 Hz; Scheme 5). Similar reactions using the

Scheme 5
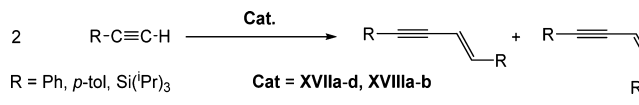
magnesium and barium bis(amide) precatalysts **XVIIa,d** under the same conditions did not result in any reactivity, while the strontium analogue **XVIIc** gave results similar to those for the calcium species (Table 7, entries 4a−c). Colorless single crystals isolated from the reaction mixture using magnesium, however, provided the structure of the polymeric acetylide complex [Mg(C≡CPh)₂(THF)]ₙ (**11**), which is the first crystallographically characterized example of an unsupported magnesium bis(acetylide) (see Figure S3 in the Supporting Information for an ORTEP representation of **11**). Conversely the calcium dialkyl precatalyst **XVIIIa** far outperformed the amide precursors: 10% conversion to the 1,3-enyne was reached after 48 h under the same conditions (Table 7, entry 4d), yielding a 9/1 mixture of the Z and the E isomers (E isomer: AB spin system at 6.25 and 6.89 ppm, $^3J_{trans}$ = 16.2 Hz). The strontium dialkyl precursor **XVIIIb** displayed very similar activity but yielded the 1,3-enyne as a 4/1 mixture of the Z and E isomers (Table 7, entry 4e). Surprisingly, repetition of the reaction in a 9/1 toluene/THF mixture led to a drastic increase in catalytic activity and allowed up to 90% conversion to be reached after 3 days at 160 °C using 5 mol % of **XVIIIa,b** (Table 7, entry 4f). A similar rate increase in polar donor solvents has already been observed in intermolecular hydro-amination reactions catalyzed by the calcium and strontium dialkyls **XVIIIa,b**.[17b] It is therefore likely that, in contrast to the formation of butatriene coupling products, which is inhibited by THF deaggregation, the mechanism for 1,3-enyne formation relies on insertion of acetylene into a monomeric THF-solvated calcium acetylide species. Although no NMR evidence could be found for an intermediate calcium butatriene diyl complex, the strong coloration of the reaction mixture suggested that such a species may be present, if only transiently in nondetectable quantities in the reaction mixture. As already noted for complex **XI**, heating a solution of isolated [Ca{C≡CPh}₂]ₙ with 4 equiv of THF in d_8-toluene for 1 day at 160 °C did not lead to any change in the ¹³C NMR shifts or provide a color change indicative of butatriene diyl formation. Addition of a further 2 equiv of phenylacetylene and heating for 18 h at 160 °C, however, provided one complete turnover to a 3/1 mixture of the E and Z isomers of the 1,3-enyne coupling product as well as a deep red coloration of the reaction mixture. Once again, ¹³C NMR analysis afforded no evidence for the presence of a calcium butatriene diyl complex.

p-Tolylacetylene also underwent selective dimerization to the corresponding 1,3-enyne but required prolonged heating at 160

°C and higher catalyst loading (10 mol %). Monitoring by ^{1}H NMR showed exclusive production of the *Z* isomer ($^3J_{cis}$ = 12.0 Hz) up to ca. 20% conversion, after which the more thermodynamically stable *E* isomer ($^3J_{trans}$ = 16.5 Hz) slowly started to form until an 1/2 equilibrium mixture of *Z* and *E* isomers was reached (Table 7, entry 5). The dimerization of triisopropylsilylacetylene proceeded much more slowly under the same conditions (Table 7, entry 6) but yielded exclusive formation of the *E* isomer of $[(^iPr)_3SiC{\equiv}CCH{=}CHSi(^iPr)_3]$ ($^3J_{trans}$ = 19.6 Hz). Simple alkylacetylenes proved much less reactive. Even after prolonged heating at 170 °C, cyclohexylacetylene and *tert*-butylacetylene did not display any reactivity (Table 7, entries 7 and 8), while a very small amount of linear 1-hexyne was converted to the corresponding butatriene $[^nBuCH{=}C{=}C{=}CH^nBu]$ (Table 7, entry 9). This observation suggests that the presence or absence of easily accessible propargylic protons determines whether calcium-mediated acetylene coupling yields the butatriene or the 1,3-enyne product. In the case of the methoxy-functionalized acetylene this mechanism is aided by precoordination of the donor oxygen atom, leading to a favorable conformation for the concerted dimerization/protonation process (vide supra).

Conclusion. A series of dimeric β-diketiminate-supported magnesium and calcium acetylides have been reported and structurally characterized. In all cases the bridging acetylide ligands were shown to coordinate in an asymmetric fashion to the alkaline-earth dications through a side-on C≡C to metal interaction, the degree of which increases with the size of the metal center and is highly dependent on the nature (steric demands, donor functionality) of the acetylide substituents. Selective head-to-head dimerization of methyl propargyl ether into the corresponding butatriene derivative was achieved using a range of heteroleptic and homoleptic calcium precursors, with optimal catalytic activity displayed by the simple bis(amido) complex $[Ca\{N(SiMe_3)_2\}_2(THF)_2]$ in the presence of catalytic amounts of THF. The reaction mechanism was investigated and is suggested to proceed via a concerted dimerization/protonolysis pathway relying on the C−H activation of the propargylic position of the alkyne. While this catalytic reactivity could not be extended to other donor-functionalized terminal acetylenes, aryl- and trialkylsilylacetylenes underwent selective calcium-catalyzed head to head dimerization to the corresponding 1,3-enynes in THF, albeit under forcing conditions. No reactivity was observed for terminal alkynes bearing secondary or tertiary alkyl substituents.

■ EXPERIMENTAL SECTION

All manipulations were carried out using standard Schlenk line and glovebox techniques under an inert atmosphere of argon. NMR experiments were conducted in J. Young tap NMR tubes made up and sealed in a glovebox. NMR spectra were recorded on a Bruker AV-400 spectrometer at 100.6 MHz (^{13}C), a Bruker AV-300 spectrometer at 75.5 MHz (^{13}C), or a Bruker AV-250 spectrometer at 62.9 MHz (^{13}C). The spectra were referenced relative to residual solvent resonances. Data quoted were recorded at 298 K. Infrared spectra were recorded as pressed KBr pellets on a Nicolet Nexus FTIR spectrometer. Elemental analyses were performed on crystalline samples prepared after removal of volatiles by exposure to a dynamic vacuum by Mr. Stephen Boyer at SACS, London Metropolitan University. Solvents (toluene, benzene, THF, hexane) were dried by passage through a commercial solvent purification system, under nitrogen and stored in ampoules over molecular sieves. C_6D_6 and d_8-toluene were purchased from Goss Scientific Instruments Ltd. and dried over molten potassium before distilling under nitrogen and storing over molecular sieves. Tetrakis-

(trimethylsilyl)silane (TMSS) was purchased from Goss Scientific Instruments Ltd. and used as received. Solid potassium hexamethyldisilylazide, CaI_2, SrI_2, and BaI_2 were purchased from Sigma-Aldrich and used as received. $[\{ArNC(Me)CHC(Me)NAr\}Ca\{N(SiMe_3)_2\}]$[24] (Ar = 2,6-diisopropylphenyl) and the homoleptic group 2 amides and alkyls $[M\{N(SiMe_3)_2\}_2]$ (M = Mg, Ca, Sr, Ba)[25] and $[M\{CH(SiMe_3)_2\}_2(THF)_2]$ (M = Mg, Ca, Sr, Ba)[26] were synthesized using literature procedures.

Synthesis and Characterization of Magnesium Acetylides $[LMgC{\equiv}CR]_2$. $[LMg\{N(SiMe_3)_2\}]$ (1.00 mmol, 602 mg) was weighed into a Schlenk tube, dissolved in benzene (5.00 mL), and then treated with alkyne (1.00 mmol). The resulting mixture was stirred at 60 °C for 60 h, by which time crystals had formed. The crystalline product $[LMgC{\equiv}CR]_2$ was isolated by filtration at room temperature.

$[LMgC{\equiv}C(CH_2)_3CH_3]_2$ (1). Yield: 395 mg, 0.75 mmol, 75%. ^{1}H NMR (d_8-toluene, 300 MHz, 298 K): δ 0.47 (d, 6H, ^3J = 6.9 Hz, ^iPr-CH_3), 0.88 (t, 3H, ^3J = 7.2 Hz, Bu-CH_3), 1.16 (d, 6H, ^3J = 6.9 Hz, ^iPr-CH_3), 1.19 (d, 6H, ^3J = 6.9 Hz, ^iPr-CH_3), 1.31 (m, 4H, Bu-CH_2), 1.44 (s, 6H, NCCH_3), 2.20 (t, 2H, ^3J = 7.2 Hz, Bu-CH_2), 3.06 (sept, 2H, ^3J = 6.8 Hz, ^iPr-CH), 3.40 (sept, 2H, ^3J = 6.8 Hz, ^iPr-CH), 4.65 (s, 1H, β-CH), 6.98–7.17 (m, 6H, Ar-H). ^{13}C{^{1}H} NMR (d_8-toluene, 77.5 MHz, 298 K): δ 13.8 (Bu-CH_3), 22.9, 24.3, 24.5, 24.9, 25.8, 27.4, 28.9, 31.2 (C≡CCH_2), 95.0 (β-CH), 112.2 (M$C_α{\equiv}C_β$), 121.0 (M$C_α{\equiv}C_β$), 123.9 (*m*-Ar-C), 124.0 (*m*-Ar-C), 125.8 (*p*-Ar-C), 142.2 (*o*-Ar-C), 143.6 (*o*-Ar-C), 146.1 (*i*-Ar-C), 169.3 (NCMe). IR (KBr): 3056, 3020, 2959, 2924, 2866, 2059, 1538, 1520, 1461, 1436, 1403, 1366, 1312, 1263, 1233, 1175, 1100, 1061, 1022, 933, 849, 795, 760 cm^{-1}. Anal. Calcd for $C_{70}H_{100}Mg_2N_4$ (M_w = 1046.2): C, 80.36; H, 9.63; N, 5.36. Found: C, 80.28; H, 9.60; N, 5.28.

$[LMgC{\equiv}C^tBu]_2$ (2). NMR scale: 40 mg of $[LMg\{N(SiMe_3)_2\}]$ (66.4 μmol) and 8.18 μL of 3,3-dimethyl-1-butyne (66.4 μmol) were heated in toluene at 80 °C for 24 h. NMR data showed quantitative conversion to **2**. Colorless crystals were isolated from the NMR tube (30 mg, 57.3 μmol, 86% yield). ^{1}H NMR (d_5-pyridine, 300 MHz, 298 K): δ = 1.12 (d, 12H, ^3J = 6.9 Hz, ^iPr-CH_3), 1.30 (s, 9H, ^tBu-CH_3), 1.36 (d, 12H, ^3J = 6.9 Hz, ^iPr-CH_3), 1.91 (s, 6H, NCCH_3), 3.39 (sept, 4H, ^3J = 6.8 Hz, ^iPr-CH), 5.09 (s, 1H, β-CH), 7.29–7.31 (m, 6H, Ar-H). ^{13}C{^{1}H} NMR (d_5-pyridine, 77.5 MHz, 298 K): δ 24.6, 24.8, 25.2, 28.8 (^tBu-CH_3), 28.9, 33.2 (^tBu-CCH$_3$), 94.7 (β-CH), 103.5 (Mg$C_α{\equiv}C_β$), 120.1 (Mg$C_α{\equiv}C_β$), 124.2 (*m*-Ar-C), 125.6 (*p*-Ar-C), 143.1 (*o*-Ar-C), 145.9 (*i*-Ar-C), 169.1 (NCMe). IR (KBr): 3056, 2961, 2926, 2866, 2038, 1561, 1539, 1522, 1464, 1437, 1398, 1365, 1313, 1260, 1175, 1102, 1055, 1020, 931, 846, 791, 760, 753 cm^{-1}. The product consistently yielded unsatisfactory elemental analysis presumably due to its air sensitivity, despite NMR data showing a single clean product. NMR spectra are provided in the Supporting Information as corroborative evidence of purity.

$[LMgC{\equiv}CCy]_2$ (3). NMR scale: 40 mg of $[LMg\{N(SiMe_3)_2\}]$ (66.4 μmol) and 8.68 μL of cyclohexylacetylene (66.4 μmol) were heated in toluene at 80 °C for 24 h. NMR data showed quantitative conversion to **3**. Colorless crystals were isolated from the NMR tube (31 mg, 56.5 μmol, 85% yield). ^{1}H NMR (d_5-pyridine, 300 MHz, 298 K): δ 1.15 (d, 12H, ^3J = 6.9 Hz, ^iPr-CH_3), 1.22–1.33 (m, 4H, Cy-H), 1.37 (d, 12H, ^3J = 6.9 Hz, ^iPr-CH_3), 1.42–1.62 (m, 2H, Cy-H), 1.70–1.79 (m, 2H, Cy-H), 1.82–1.89 (m, 2H, Cy-H), 1.92 (s, 6H, NCCH_3), 2.45 (m, 1H, Cy-CH), 3.42 (sept, 4H, ^3J = 6.8 Hz, ^iPr-CH), 5.10 (s, 1H, β-CH), 7.30–7.33 (m, 6H, Ar-H). ^{13}C{^{1}H} NMR (d_5-pyridine, 77.5 MHz, 298 K): δ 24.7, 24.8, 25.3, 25.6, 27.2, 29.0, 31.8, 35.0 (Cy-CH), 94.7 (β-CH), 105.8 (Mg$C_α{\equiv}C_β$), 115.4 (Mg$C_α{\equiv}C_β$), 124.3 (*m*-Ar-C), 125.7 (*p*-Ar-C), 143.1 (*o*-Ar-C), 145.9 (*i*-Ar-C), 169.2 (NCMe). IR (KBr): 3056, 3015, 2957, 2927, 2864, 2849, 2048, 1523, 1463, 1435, 1400, 1361, 1315, 1258, 1174, 1103, 1059, 1019, 927, 888, 850, 793, 761, 753 cm^{-1}. Anal. Calcd for $C_{74}H_{104}Mg_2N_4$ (M_w = 1098.3): C, 80.93; H, 9.54; N, 5.10. Found: C, 80.86; H, 9.59; N, 5.19.

$[LMgC{\equiv}CPh]_2$ (4). Yield: 365 mg, 0.67 mmol, 67%. ^{1}H NMR (d_8-toluene, 300 MHz, 298 K): δ 0.34 (d, 6H, ^3J = 6.9 Hz, ^iPr-CH_3), 0.79 (d, 6H, ^3J = 6.9 Hz, ^iPr-CH_3), 1.26 (d, 6H, ^3J = 6.9 Hz, ^iPr-CH_3), 1.50 (s, 6H, NCCH_3), 1.60 (d, 6H, ^3J = 6.9 Hz, ^iPr-CH_3), 2.97 (sept, 2H, ^3J = 6.8 Hz, ^iPr-CH), 3.52 (sept, 2H, ^3J = 6.8 Hz, ^iPr-CH), 5.01 (s, 1H β-

CH), 6.87–7.68 (m, 11H, Ar-*H*). ^{13}C{^{1}H} NMR (d_5-pyridine, 77.5 MHz, 298 K): δ 24.7, 25.1, 29.1, 94.9 (β-CH), 111.2 (MgC$_\alpha$≡C$_\beta$), 122.0 (MgC$_\alpha$≡C$_\beta$), 124.4 (*m*-Ar-*C*), 125.8 (*p*-Ar-*C*), 126.2 (*p*-Ph-*C*), 128.6 (*m*-Ph-*C*), 129.0 (*i*-Ph-*C*), 132.3 (*o*-Ph-*C*), 143.3 (*o*-Ar-*C*), 145.7 (*i*-Ar-*C*), 169.4 (N*C*Me). IR (KBr): 3057, 2959, 2923, 2046, 1559, 1539, 1521, 1465, 1457, 1437, 1403, 1364, 1317, 1259, 1180, 1069, 1059, 1019, 929, 852, 793, 763, 755, 692 cm^{-1}. Anal. Calcd for C$_{74}$H$_{92}$Mg$_2$N$_4$ (M_w = 1086.2): C, 81.83; H, 8.54; N, 5.16. Found: C, 81.79; H, 8.60; N, 5.08.

[LMgC≡C(4-MePh)]₂ (5). NMR scale: 40 mg of [LMg{N-(SiMe$_3$)$_2$}] (66.4 μmol) and 7.71 mg of p-tolylacetylene (66.4 μmol) were heated in toluene at 80 °C for 24 h. NMR data showed quantitative conversion to **5**. Colorless crystals were isolated from the NMR tube (34 mg, 61.0 μmol, 92% yield). ^{1}H NMR (d_5-pyridine, 300 MHz, 298 K): δ 1.13 (d, 12H, ^3J = 6.9 Hz, ^{i}Pr-CH$_3$), 1.36 (d, 12H, ^3J = 6.9 Hz, ^{i}Pr-CH$_3$), 1.91 (s, 6H, NCCH$_3$), 2.12 (s, 3H, tol-CH$_3$), 3.46 (sept, 4H, ^3J = 6.8 Hz, ^{i}Pr-CH), 5.11 (s, 1H, β-CH), 6.92 (d, 2H, ^3J = 7.8 Hz, *o*-tol-*H*), 7.29–7.30 (m, 6H, Ar-*H*), 7.42 (d, 2H, ^3J = 7.8 Hz, *o*-tol-*H*). ^{13}C{^{1}H} NMR (d_5-pyridine, 77.5 MHz, 298 K): δ 21.6 (tol-CH$_3$), 24.6, 24.8, 25.1, 29.1, 94.8 (β-CH), 115.3 (MgC$_\alpha$≡C$_\beta$), 124.4 (*m*-Ar-*C*), 125.4 (MgC$_\alpha$≡C$_\beta$), 125.8 (*p*-Ar-*C*), 129.2 (*m*-tol-*C*), 132.3 (*o*-tol-*C*), 135.3 (*p*-tol-*C*), 138.1 (*i*-tol-*C*), 143.2 (*o*-Ar-*C*), 145.7 (*i*-Ar-*C*), 169.3 (N*C*Me). IR (KBr): 3062, 2961, 2923, 2866, 2052, 1622, 1540, 1521, 1463, 1437, 1404, 1363, 1315, 1262, 1176, 1102, 1057, 1020, 930, 850, 818, 794, 761, 751, 710 cm^{-1}. Anal. Calcd for C$_{76}$H$_{96}$Mg$_2$N$_4$ (M_w = 1114.2): C, 81.92; H, 8.68; N, 5.03. Found: C, 82.01; H, 8.59; 5.13.

[LMgC≡CCH₂OMe]₂ (6). Yield: 250 mg, 0.49 mmol, 49%. ^{1}H NMR (d_8-toluene, 300 MHz, 298 K): δ 0.47 (d, 6H, ^3J = 6.6 Hz, ^{i}Pr-CH$_3$), 1.15 (d, 6H, ^3J = 6.6 Hz, ^{i}Pr-CH$_3$), 1.18 (d, 6H, ^3J = 6.6 Hz, ^{i}Pr-CH$_3$), 1.42 (s, 6H, NCCH$_3$), 1.44 (d, 6H, ^3J = 6.6 Hz, ^{i}Pr-CH$_3$), 3.00 (sept, 2H, ^3J = 6.6 Hz, ^{i}Pr-CH), 3.16 (s, 3H, OCH$_3$), 3.35 (sept, 2H, ^3J = 6.6 Hz, ^{i}Pr-CH), 3.94 (s, 2H, OCH$_2$), 4.60 (s, 1H, β-CH), 6.97–7.15 (m, 6H, Ar-*H*). ^{13}C{^{1}H} NMR (d_8-toluene, 77.5 MHz, 298 K): δ 24.2, 24.3, 24.4, 24.9, 25.9, 27.4, 29.0, 57.7 (OCH$_3$), 60.8 (OCH$_2$), 95.0 (β-CH), 115.6 (MC$_\alpha$≡C$_\beta$), 120.4 (MC$_\alpha$≡C$_\beta$), 123.8 (*m*-Ar-*C*), 124.2 (*m*-Ar-*C*), 125.8 (*p*-Ar-*C*), 142.0 (*o*-Ar-*C*), 143.7 (*o*-Ar-*C*), 145.6 (*i*-Ar-*C*), 169.5 (N*C*Me). IR (KBr): 3057, 3018, 2961, 2917, 2814, 2026, 1538, 1523, 1460, 1434, 1403, 1365, 1313, 1264, 1231, 1178, 1104, 1060, 1022, 928, 900, 808, 759, 759 cm^{-1}. The product consistently yielded unsatisfactory elemental analysis, despite NMR data showing a single clean product. NMR spectra are provided in the Supporting Information as corroborative evidence of purity.

[LMgC≡CCH₂OPh]₂ (7). Yield: 400 mg, 0.70 mmol, 70%. ^{1}H NMR (d_8-toluene, 300 MHz, 298 K): δ 0.46 (d, 6H, ^3J = 6.6 Hz, ^{i}Pr-CH$_3$), 1.11 (d, 6H, ^3J = 6.6 Hz, ^{i}Pr-CH$_3$), 1.15 (d, 6H, ^3J = 6.6 Hz, ^{i}Pr-CH$_3$), 1.32 (d, 6H, ^3J = 6.6 Hz, ^{i}Pr-CH$_3$), 1.43 (s, 6H, NCCH$_3$), 3.02 (sept, 2H, ^3J = 6.6 Hz, ^{i}Pr-CH), 3.26 (sept, 2H, ^3J = 6.6 Hz, ^{i}Pr-CH), 4.61 (s, 2H, OCH$_2$), 4.65 (s, 1H, β-CH), 6.81–7.10 (m, 11H, Ar/OPh-*H*). ^{13}C{^{1}H} NMR (d_8-toluene, 77.5 MHz, 298 K): δ 24.2, 24.3, 24.5, 24.9, 26.0, 27.5, 29.0, 56.0 (OCH$_2$), 95.0 (β-CH), 114.7 (*o*-Ph-*C*), 115.1 (MC$_\alpha$≡C$_\beta$), 120.1 (MC$_\alpha$≡C$_\beta$), 121.3 (*p*-Ph-*C*) 124.0 (*m*-Ar-*C*), 124.2 (*m*-Ar-*C*), 126.0 (*p*-Ar-*C*), 129.7 (*m*-Ph-*C*), 142.1 (*o*-Ar-*C*), 143.6 (*o*-Ar-*C*), 145.3 (*i*-Ar-*C*), 158.6 (*i*-Ph-*C*), 170.0 (N*C*Me). IR (KBr): 3055, 3022, 2956, 2925, 2862, 2027, 1600, 1588, 1533, 1493, 1462, 1438, 1403, 1365, 1315, 1266, 1230, 1217, 1177, 1104, 1078, 1034, 1022, 930, 849, 794, 759, 749, 690 cm^{-1}. Anal. Calcd for C$_{76}$H$_{96}$Mg$_2$N$_4$O$_2$ (M_w = 1146.2): C, 79.64; H, 8.44; N, 4.89. Found: C, 79.59; H, 8.50; N, 4.86.

[LMgC≡CCH₂NMe₂]₂ (8). Yield: 490 mg, 0.93 mmol, 93%. ^{1}H NMR (d_5-pyridine, 300 MHz, 298 K): δ 1.01 (d, 12H, ^3J = 6.6 Hz, ^{i}Pr-CH$_3$), 1.21 (d, 12H, ^3J = 6.6 Hz, ^{i}Pr-CH$_3$), 1.08 (s, 6H, NCCH$_3$), 2.08 (s, 6H, NCH$_3$), 3.09 (s, 2H, NCH$_2$), 3.28 (sept, 2H, ^3J = 6.6 Hz, ^{i}Pr-CH), 5.03 (s, 1H, CH), 7.20–7.23 (m, 6H, Ar-*H*). ^{13}C{^{1}H} NMR (d_5-pyridine, 77.5 MHz, 298 K): δ 24.6, 25.2, 27.0, 44.5 (NCH$_3$), 50.8 (NCH$_2$), 94.8 (β-CH), 104.7 (MC$_\alpha$≡C$_\beta$), 112.9 (MC$_\alpha$≡C$_\beta$), 125.7 (*p*-Ar-*C*), 129.2 (*o*-Ar-*C*), 143.2 (*m*-Ar-*C*), 145.8 (*i*-Ar-*C*), 169.3 (N*C*Me). IR (KBr): 3054, 3019, 2955, 2865, 2815, 2780, 2758, 2030, 1539, 1523, 1464, 1438, 1403, 1366, 1315, 1260, 1232, 1177, 1102, 1035, 1019, 929, 851, 792, 760 cm^{-1}. The product consistently yielded

unsatisfactory elemental analysis, despite NMR data showing a single clean product. NMR spectra are provided to prove purity.

Synthesis and Characterization of Calcium Acetylides [LCaC≡CR]₂. [LCa{N(SiMe$_3$)$_2$}(THF)] (0.73 mmol, 500 mg) was weighed into a Schlenk tube, dissolved in toluene (5.00 mL), and then treated with alkyne (0.73 mmol). The resulting mixture was stirred at room temperature for 2 h. The crystalline product [LCaC≡CR]₂ was isolated after cooling to 4 °C for 48 h.

[LCaC≡CCH₂OPh]₂ (9). Yield: 0.30 g, 0.51 mmol, 70%. ^{1}H NMR (C$_6$D$_6$, 300 MHz, 298 K): δ 1.18 (d, 12H, ^{i}Pr-CH$_3$, ^3J = 6.8 Hz), 1.27 (d, 12H, ^{i}Pr-CH$_3$, ^3J = 6.8 Hz), 1.70 (s, 6H, NCCH$_3$), 3.30 (sept, 4H, ^{i}Pr-CH, ^3J = 6.8 Hz), 3.89 (s, 2H, OCH$_2$), 4.95 (s, 1H, β-CH), 6.86–6.94 (m, 3H, Ar/Ph-*H*), 7.13–7.21 (m, 7H, Ar/Ph-*H*). ^{13}C{^{1}H} NMR (C$_6$D$_6$, 75 MHz, 298K): δ 20.8, 24.3, 28.6, 60.0 (OCH$_2$), 94.3 (β-CH), 106.3 (CaC$_\alpha$≡C$_\beta$), 115.5 (*o*-Ph-*C*), 124.0 (*p*-Ph-*C*), 124.2 (*m*-Ar-*C*), 124.8 (*p*-Ar-*C*), 130.0 (*m*-Ph-*C*), 142.4 (*o*-Ar-*C*), 146.1 (*i*-Ar-*C*), 148.6 (CaC$_\alpha$≡C$_\beta$), 156.6 (*i*-Ph-*C*), 165.6 (N*C*Me). IR (KBr): 3051, 3017, 2961, 2922, 2863, 2074, 1599, 1590, 1547, 1510, 1492, 1461, 1431, 1406, 1365, 1314, 1265, 1251, 1225, 1201, 1167, 1099, 1015, 975, 923, 828, 784, 751, 690 cm^{-1}. Anal. Calcd for C$_{76}$H$_{96}$Ca$_2$N$_4$O$_2$ (M_w = 1177.8): C, 77.50; H, 8.22; N, 4.76. Found: C, 77.42; H, 8.34; N, 4.64.

[LCaC≡CCH₂NMe₂]₂ (10). Yield: 0.28 g, 0.52 mmol, 71%. ^{1}H NMR (C$_6$D$_6$, 300 MHz, 298 K): δ 1.21 (d, 12H, ^{i}Pr-CH$_3$, ^3J = 6.8 Hz), 1.23 (d, 12H, ^{i}Pr-CH$_3$, ^3J = 6.8 Hz), 1.66 (s, 6H, NCCH$_3$), 1.89 (s, 6H, NCH$_3$), 2.57 (s, 2H, NCH$_2$), 3.30 (sept, 4H, ^{i}Pr-CH, ^3J = 6.8 Hz), 4.80 (s, 1H, β-CH), 7.16–7.18 (m, 6H, Ar-*H*); ^{13}C{^{1}H} NMR (C$_6$D$_6$, 75 MHz, 298 K): δ 20.8, 24.5, 28.7, 60.2 (NCH$_3$), 61.0 (NCH$_2$), 92.0 (β-CH), 102.8 (CaC$_\alpha$≡C$_\beta$), 123.6 (*m*-Ar-*C*), 125.8 (*p*-Ar-*C*), 135.0 (CaC$_\alpha$≡C$_\beta$), 142.8 (*o*-Ar-*C*), 146.8 (*i*-Ar-*C*), 164.1 (N*C*Me). IR (KBr): 3050, 3019, 2959, 2924, 2864, 2815, 1775, 2027, 1542, 1516, 1459, 1435, 1399, 1364, 1314, 1267, 1251, 1225, 1170, 1100, 1021, 930, 889, 841, 788, 758 cm^{-1}. Anal. Calcd for C$_{68}$H$_{98}$Ca$_2$N$_6$ (M_w = 1079.7): C, 75.64; H, 9.15; N, 7.78. Found: C, 75.62; H, 9.16; N, 7.69.

Group 2 Mediated Coupling of Terminal Acetylenes. Inside a glovebox 20 μmol of precatalyst and 80 μmol of THF were dissolved in 0.25 mL of d_8-toluene and transferred into a J. Young tap NMR tube. A 0.4 mmol portion of acetylene was then dissolved in 0.25 mL of d_8-toluene and added to the precatalyst solution. The resulting reaction mixture was sealed and heated to 80–160 °C while being regularly monitored by ^{1}H NMR until no further conversion to the coupled product was observed.

[MeOCH₂CH=C=C=CHCH₂OMe]. ^{1}H NMR (d_8-toluene, 300 MHz, 298 K): δ 3.17 (s, 6H, CH$_3$), 5.24 (d, 4H, CH$_2$, ^3J = 6.0 Hz), 6.71 (t, 2H, CH, ^3J = 6.0 Hz). ^{13}C{^{1}H} NMR (d_8-toluene, 75 MHz, 298K): δ 55.5 (OCH$_3$), 90.0 (OCH$_2$), 123.4 (HC=C), 201.8 (HC=C). ESI-MS (*m/z*) for [C$_8$H$_{12}$O$_2$ − Na]$^+$: found 152.9888, calcd 152.9953.

[PhOCH₂CH=C=C=CHCH₂OPh]. Stoichiometric reactivity only. ^{1}H NMR (C$_6$D$_6$, 300 MHz, 298 K): δ 5.06 (d, 4H, CH$_2$, ^3J = 5.5 Hz), 6.65 (t, 2H, CH, ^3J = 5.5 Hz), 6.78–7.10 (m, 10H, Ph-*H*). ESI-MS (*m/z*) for [C$_{18}$H$_{16}$O$_2$ − Na]$^+$: 287.1068, calcd 287.1048.

[Me₂NCH₂CH=C=C=CHCH₂NMe₂]. Stoichiometric reactivity only. ^{1}H NMR (d_8-toluene, 300 MHz, 298 K): δ 2.24 (s, 12H, N(CH$_3$)$_2$), 5.24 (d, 4H, NCH$_2$, ^3J = 5.8 Hz), 5.92 (t, 2H, CH, ^3J = 5.8 Hz).

[PhC≡CCH=CHPh]. 90% yield, 90% Z isomer, 10% E isomer by NMR. ^{1}H NMR of Z isomer (d_8-toluene/THF 9/1, 300 MHz, 298 K): δ 5.76 (d, 1H, CH, $^3J_{cis}$ = 11.7 Hz), 6.46 (d, 1H, CH, $^3J_{cis}$ = 11.7 Hz), 7.05–7.09 (m, 4H, Ph-*H*), 7.17 (two overlapping d, 2H, Ph-*H*, ^3J = 7.8, 7.2 Hz), 7.35 (two overlapping d, 2H, ^3J = 7.8, 7.2 Hz), 7.83 (d, 2H, ^3J = 7.5 Hz). ^{1}H NMR of E isomer (d_8-toluene/THF 9/1, 300 MHz, 298 K): δ 6.26 (d, 1H, CH, $^3J_{trans}$ = 16.2 Hz), 6.88 (d, 1H, CH, $^3J_{trans}$ = 16.2 Hz), 7.05–7.09 (m, 6H, *m/p*-Ph-*H*), 7.16 (d, 2H, ^3J = 7.0 Hz, *o*-Ph-*H*), 7.36 (dd, 2H, ^3J = 8.0 Hz, ^4J = 1.5 Hz, *o*-Ph-*H*). ^{13}C{^{1}H} NMR of Z isomer (d_8-toluene/THF 9/1, 75 MHz, 298 K): δ 88.9 (PhC≡C), 96.4 (PhC≡C), 107.6 (PhCH=CH), 124.1 (*i*-Ph-*C*), 128.6, 128.7 (*p*-Ph-*C*), 128.8, 128.9 (*p*-Ph-*C*), 129.4, 131.8, 137.2 (*i*-Ph-*C*), 139.1 (PhCH=CH). ^{13}C{^{1}H} NMR of E isomer (d_8-toluene/ THF 9/1, 75 MHz, 298 K): δ 90.1 (PhC≡C), 92.8 (PhC≡C), 109.1

(PhCH=CH), 124.8 (*i*-Ph-*C*), 127.2, 129.2, 129.5, 129.8, 132.3, 132.4, 137.4 (*i*-Ph-*C*), 142.2 (PhCH=CH).

[(p-tol)C≡CCH=CH(p-tol)]. 80% yield, 64% *E* isomer, 36% *Z* isomer. ^{1}H NMR of *E* isomer (d_8-toluene/THF 9/1, 300 MHz, 298 K): δ 2.03 (s, 3H, C*H$_3$*), 2.06 (s, 3H, C*H$_3$*), 6.23 (d, 1H, C*H*, $^3J_{trans}$ = 16.1 Hz), 6.83 (d, 2H, ^3J = 7.9 Hz, *m*-tol-*H*), 6.90 (d, 1H, C*H*, $^3J_{trans}$ = 16.1 Hz), 7.03 (d, 2H, ^3J = 8.5 Hz, *m*-tol-*H*), 7.35 (d, 2H, ^3J = 7.9 Hz, *o*-tol-*H*), 7.81 (d, 2H, ^3J = 8.5 Hz, *o*-tol-*H*). ^{1}H NMR of *Z* isomer (d_8-toluene/THF 9/1, 300 MHz, 298 K): δ 2.02 (s, 3H, C*H$_3$*), 2.09 (s, 3H, C*H$_3$*), 5.72 (d, 1H, C*H*, $^3J_{cis}$ = 11.7 Hz), 6.40 (d, 1H, C*H*, $^3J_{cis}$ = 11.7 Hz), 6.83 (d, 2H, ^3J = 7.6 Hz, *m*-tol-*H*), 6.96 (d, 2H, ^3J = 7.6 Hz, *m*-tol-*H*), 7.33 (d, 2H, ^3J = 7.6 Hz, *o*-tol-*H*), 7.81 (d, 2H, ^3J = 7.6 Hz, *o*-tol-*H*). ^{13}C{^{1}H} NMR of *E* isomer (d_8-toluene/THF 9/1, 75 MHz, 298 K): δ 21.1 (*C*H$_3$), 82.3 (tol*C*≡C), 92.3 (tol*C*≡C), 107.7 (tol*C*H=CH), 121.4, 126.5, 129.2, 129.6, 131.7, 134.2, 138.4, 138.7, 141.2 (tol*C*H=CH). ^{13}C{^{1}H} NMR of *Z* isomer (d_8-toluene/THF 9/1, 75 MHz, 298 K): δ 21.3 (*C*H$_3$), 88.6 (tol*C*≡C), 96.5 (tol*C*≡C), 106.7 (tol*C*H=CH), 121.3, 129.2, 129.4, 131.6, 132.3, 134.6, 138.1, 138.7 (tol*C*H=CH).

[(^{i}Pr)$_3$SiC≡CCH=CHSi(^{i}Pr)$_3$]. 35% yield, 100% *E* isomer. ^{1}H NMR (d_8-toluene, 300 MHz, 298 K): δ 0.90−0.92 (m, 6H, ^{i}Pr-C*H*), 1.06−1.12 (m, 36H, ^{i}Pr-C*H$_3$*), 6.06 (d, 1H, C*H*, $^3J_{trans}$ = 19.6 Hz), 6.48 (d, 1H, C*H*, $^3J_{trans}$ = 19.6 Hz). ^{13}C{^{1}H} NMR (d_8-toluene, 75 MHz, 298 K): δ 11.1, 11.8, 18.6, 18.9, 90.9 (Si*C*≡C), 95.8 (Si*C*≡C), 126.5 (Si*C*H=CH), 141.2 (Si*C*H=CH).

X-ray Crystallography. Data for **2**, **4**, **6**, **7**, **9**, and **10** were collected at 150 K on a Nonius KappaCCD diffractometer ($λ$(Mo K$α$) = 0.71073 Å), solved by direct methods, and refined against all F^2 values using SHELXL-97 with non-hydrogen atoms anisotropic and hydrogen atoms in the riding mode.[27] In structures **2**, **4**, **9**, and **10**, the asymmetric unit was seen to contain half of a dimer molecule proximate to a crystallographic inversion center. For compound **6** the motif was seen to contain one-fourth of a molecule (the remainder of which arises by virtue of a mirror plane and 2-fold rotation axes present in the space group symmetry), while for **7** it was seen to contain independent dimer halves. The phenoxy ligand in one of the latter (based on O1) exhibits disorder in a 65/35 ratio. Solvent was noted in the asymmetric units of **2** (one molecule of toluene), **7** (half of a benzene moiety modeled over two sites in a disorder ratio of 60/40), and **10** (half of a benzene molecule). Solvent in the motif of **6**, which totals one benzene molecule per magnesium-containing dimer, manifested itself as five fractional occupancy carbon atoms that were treated isotropically. Of these, C42−C45 were all seen to be close to a 2-fold rotation axis, while C41 was observed to be coincident with this axis. Inclusion of the hydrogen atom associated with C45 was precluded by a combination of the disorder and symmetry pertaining to C41. Pseudomerohedral twinning of 25% about the 0,−1,1 reciprocal vector was accounted for in the model of **10**.

■ ASSOCIATED CONTENT

Ⓢ Supporting Information

Figures, tables, and CIF files giving ORTEP representations and crystallographic details for compounds **1**, **8**, and **11**, crystallographic data for **2**, **4**, **6**, **7**, **9**, and **10**, and NMR spectra for compounds **2**, **6**, and **8**. This material is available free of charge via the Internet at http://pubs.acs.org.

■ AUTHOR INFORMATION

Corresponding Author
*E-mail for M.S.H.: m.s.hill@bath.ac.uk.

Notes
The authors declare no competing financial interest.

■ ACKNOWLEDGMENTS

■ REFERENCES

(1) Coles, M. A.; Hart, F. A. *J. Organomet. Chem.* **1971**, *32* (3), 279.

(2) Burkey, D. J.; Hanusa, T. P. *Organometallics* **1996**, *15* (23), 4971.

(3) Green, D. C.; Englich, U.; Ruhlandt-Senge, K. *Angew. Chem., Int. Ed.* **1999**, *38* (3), 354.

(4) Guino-o, M. A.; Alexander, J. S.; McKee, M. L.; Hope, H.; Englich, U. B.; Ruhlandt-Senge, K. *Chem. Eur. J.* **2009**, *15* (44), 11842.

(5) Avent, A. G.; Crimmin, M. R.; Hill, M. S.; Hitchcock, P. B. *Organometallics* **2005**, *24* (6), 1184.

(6) Barrett, A. G. M.; Crimmin, M. R.; Hill, M. S.; Hitchcock, P. B.; Lomas, S. L.; Mahon, M. F; Procopiou, P. A.; Suntharalingam, K. *Organometallics* **2008**, *27*, 6300.

(7) Stasch, A.; Sarish, S. P.; Roesky, H. W.; Meindl, K.; Dall'Antonia, F.; Schulz, T.; Stalke, D. *Chem Asian J.* **2009**, *4* (9), 1451.

(8) Barrett, A. G. M.; Crimmin, M. R.; Hill, M. S.; Hitchcock, P. B.; Lomas, S. L.; Procopiou, P. A.; Suntharalingam, K. *Chem. Commun.* **2009**, 2299.

(9) Arrowsmith, M.; Crimmin, M. R.; Barrett, A. G. M.; Hill, M. S.; Kociok-Köhn, G.; Procopiou, P. A. *Organometallics* **2011**, *30* (6), 1493.

(10) Thompson, M. E.; Baxter, S. M.; Bulls, A. R.; Burger, B. J.; Nolan, M. C.; Santarsiero, B. D.; Schaefer, W. P.; Bercaw, J. E. *J. Am. Chem. Soc.* **1987**, *109*, 203.

(11) Den Haan, K. H.; Wielstra, Y.; Teuben, J. H. *Organometallics* **1987**, *6*, 2053.

(12) (a) Heeres, H. J.; Nijhoff, J.; Teuben, J. H. *Organometallics* **1993**, *12*, 2609. (b) Heeres, H. J.; Teuben, J. H. *Organometallics* **1991**, *10*, 1980. (c) Komeyama, K.; Takehira, K.; Takaki, K. *Synthesis* **2004**, *7*, 1062. (d) Komeyama, K.; Kawabata, T.; Takehira, K.; Takaki, K. *J. Org. Chem.* **2005**, *70*, 7260. (e) Ge, S.; Quiroga Norambuena, V. F.; Hessen, B. *Organometallics* **2007**, *26*, 6508.

(13) Nishiura, M.; Hou, Z.; Wakatsuki, Y.; Yamaki, T.; Miyamoto, Ta. *J. Am. Chem. Soc.* **2003**, *125*, 1184.

(14) (a) Straub, T.; Haskel, A.; Eisen, M. S. *J. Am. Chem. Soc.* **1995**, *117*, 6364. (b) Eisen, M. S.; Straub, T.; Haskel, A. *J. Alloys Compd.* **1998**, *271*, 116. (c) Haskel, A.; Wang, J. Q.; Straub, T.; Neyroud, T. G.; Eisen, M. S. *J. Am. Chem. Soc.* **1999**, *121*, 3025. (d) Dash, A. K.; Wang, J. X.; Berthet, J.-C.; Ephritikhine, M.; Eisen, M. S. *J. Organomet. Chem.* **2000**, *604*, 83. (e) Dash, A. K.; Gourevich, I.; Wang, J. Q.; Wang, J.; Kapon, M.; Eisen, M. S. *Organometallics* **2001**, *20*, 5084. (f) Wang, J. Q.; Eisen, M. S. *J. Organomet. Chem.* **2003**, *670*, 97.

(15) Chang, C. C.; Srinivas, B.; Wu, M. L.; Chiang, W. H.; Chiang, M. Y.; Hsiung, C. S. *Organometallics* **1995**, *14* (11), 5150.

(16) See, for example: (a) Bell, N. A.; Nowell, I. W.; Shearer, H. M. M. *J. Chem. Soc., Chem. Commun.* **1982**, 147. (b) Yang, K.; Chang, C.; Huang, J.; Lin, C.; Lee, G.; Wang, Y.; Chiang, M. Y. *J. Organomet. Chem.* **2002**, *648*, 176. (c) Evans, W. J.; Bloom, I.; Hunter, W. E.; Atwood, J. L. *Organometallics* **1983**, *2*, 709. (d) Atwood, J. L.; Hunter, W. E.; Wayda, A. L.; Evans, W. J. *Inorg. Chem.* **1981**, *20*, 4115.

(17) (a) Schumann, H.; Steffens, A.; Hummert, M. *Z. Anorg. Allg. Chem.* **2009**, *635*, 1041. (b) Garcia-Alvarez, J.; Graham, D. V.; Hevia, E.; Kennedy, A. R.; Mulvey, R. E. *Dalton Trans.* **2008**, 1481.

(18) Arrowsmith, M.; Hill, M. S.; Kociok-Köhn, G. *Organometallics* **2011**, *30* (6), 1291.

(19) (a) Barrett, A. G. M.; Brinkmann, C.; Crimmin, M. R.; Hill, M. S.; Hunt, P.; Procopiou, P. A. *J. Am. Chem. Soc.* **2009**, *131*, 12906. (b) Brinkmann, C.; Barrett, A. G. M.; Hill, M. S.; Procopiou, P. A. *J. Am. Chem. Soc.* **2012**, *134*, 2193.

(20) (a) Auffrant, A.; Jaun, B.; Jarowski, P. D.; Houk, K. N.; Diederich, F. *Chem. Eur. J.* **2004**, *10*, 2906. (b) Jarowski, P. D.; Diederich, F.; Houk, K. N. *J. Phys. Chem.* **2006**, *110*, 7237.

(21) (a) Forsyth, C. M.; Nolan, S. P.; Stern, C. L.; Marks, T. J. *Organometallics* **1993**, *12*, 3618. (b) Evans, W. J.; Keyer, R. A.; Ziller, J. W. *Organometallics* **1993**, *12*, 2618. (c) Evans, W. J.; Keyer, R. A.; Zhang, H. M.; Atwood, J. L. *J. Chem. Soc., Chem. Commun.* **1987**, 837. (d) Evans, W. J.; Keyer, R. A.; Ziller, J. W. *Organometallics* **1990**, *9*, 2628.

(22) Dunne, J. F.; Fulton, D. B.; Ellern, A.; Sadow, A. D. *J. Am. Chem. Soc.* **2010**, *132* (50), 17680.

(23) (a) Liu, B.; Roisnel, T.; Carpentier, J.-F.; Sarazin, Y. *Angew. Chem., Int. Ed.* **2012**, *51*, 4943. (b) Zhang, X. M.; Emge, T. J.; Hultzsch, K. C. *Angew. Chem., Int. Ed.* **2012**, *51*, 394.

(24) Crimmin, M. R.; Hill, M. S.; Hitchcock, P. B.; Mahon, M. F. *New J. Chem.* **2010**, 1572.

(25) Westerhausen, M. *Inorg. Chem.* **1991**, *30*, 96.

(26) Crimmin, M. R.; Barrett, A. G. M.; Hill, M. S.; MacDougall, D. J.; Mahon, M. F.; Procopiou, P. A. *Chem. Eur. J.* **2008**, *14*, 11292.

(27) Sheldrick, G. M. *SHELXL-97, Program for the Refinement of Crystal Structures*; University of Göttingen, Göttingen, Germany, 1997.